International Journal of Environmental Sciences
ISSN: 2229-7359
Vol. 11 No. 2s, 2025
https://www.theaspd.com/ijes.php

Antifungal Effectiveness Of Silver-Substituted Copper Ferrite Nanopowder Produced By Sol-Gel Synthesis

Sheryil Malvilayil[a] **Manish Fukate**[b]

a) Research Scholar, Department of Chemistry, G H Raisoni University, Amravati , MS (India)
E mail ID: mavilayils@gmail.com

b) Supervisor , Department of Chemistry, G H Raisoni University, Amravati , MS India

Corresponding author : manishfukate12@gmail.com

ABSTRACT

Silver-doped $CuFe_2O_4$ nanoparticles were synthesized using a sol-gel method involving citric acid at ambient temperature. The structure and microstructure of the Ag-doped $CuFe_2O_4$ nanoparticles were analyzed in relation to calcination temperature. Characterization of the synthesized nanoparticles was carried out using X-ray diffraction (XRD), Fourier transform infrared spectroscopy (FTIR), and transmission electron microscopy (TEM), which were used to confirm the formation of crystalline nanosized Ag-doped $CuFe_2O_4$ spinel. The XRD analysis revealed a crystalline inverse spinel structure with a particle size of 15.23 nm, characterized by sharp peaks that indicated a homogeneous single-phase ferrite. The antimicrobial properties of the Ag-doped $CuFe_2O_4$ nanoparticles were evaluated against three types of fungi, demonstrating significant antifungal activity. Data clearly indicate that $CuFe_2O_4$ nanoparticles with silver doping levels of 1 wt%, 2 wt%, and 3 wt% show enhanced antifungal efficacy compared to pure $CuFe_2O_4$. Additionally, the antifungal assay results exhibited superior inhibition from the doped samples versus the pure samples. Ag-doped copper ferrite shows considerable antimicrobial potential and may be applicable for medicinal uses.

Keywords: *Nanoparticles, Spinel ferrites, XRD, FTIR, Fungal pathogens.*

INTRODUCTION:

Nanosized ferrite materials have gained significant interest recently due to their unique physical and chemical properties, which differ substantially from those of traditional materials [1]. Recent research has demonstrated the antimicrobial effectiveness of various nanoparticles, including those made from silver [2], copper [3] , titanium dioxide, and zinc oxide. Historically, metals and their compounds have served as therapeutic agents, and current materials science research is focused on discovering new materials with improved properties [5]. Transition metals such as copper, zinc, chromium, and nickel have shown prominent antimicrobial characteristics. Some researchers propose that metal substitution in spinel structures may enhance the biomedical properties of ferrite nanoparticles [6]. Magnetic nanoparticles are particularly promising because their large surface area to volume ratio offers exceptional antibacterial traits, drawing attention to researchers in light of rising microbial resistance to antibiotics and the emergence of resistant strains[7-9]. Consequently, various methods—including solid-state reactions [10], co-precipitation[11], hydrothermal [12],ceramic processes [13] and sol-gel techniques—have yielded interesting findings regarding the synthesis of nanosized magnetic spinel ferrite nanoparticles and the influence of dopants on their magnetic and antibacterial properties. Among these, we chose the sol-gel method because it can produce a significant quantity of product in a short time. This low-temperature technique results in a three-dimensional inorganic network [15]. As noted, there has been limited literature on silver-doped copper ferrite systems and their antibacterial activities. Thus, this study aims to explore the effect of doping on both the structural and antibacterial properties of copper-zinc ferrite nanoparticles synthesized via the sol-gel method.

MATERIALS AND METHODS: Copper nitrate tetrahydrate, iron nitrate nonhydrate, citric acid, and silver nitrate $Ag(NO_3)_2{\cdot}4H_2O$) were obtained in analytical grade. All experiments were conducted with ethyl alcohol. Both undoped and silver-doped $CuFe_2O_4$ were synthesized through the sol-gel technique.

SYNTHESIS OF $CUFE_2O_4$ NANOPARTICLE:
The synthesis of silver-doped $CuFe_2O_4$ nanoparticles employed the sol-gel method. All reagents were added to a beaker and stirred continuously at 80°C for 2 hours until a gel was formed. This gel was then heated in a pressure bomb at 131°C for 12 hours and subsequently calcined at 350°C.

ASSAY FOR EVALUATING ANTIFUNGAL ACTIVITY: FUNGAL CULTURE:

Test Organisms: Aspergillus, Aspergillus flavus Potato dextrose broth served as the medium for the disc diffusion assay.

PREPARATION OF FUNGAL SUSPENSION:
Using a sterile wire loop, the fungal test was inoculated in a test tube containing potato dextrose broth. The inoculum concentration was adjusted to 0.5 McFarland's standards, equivalent to 10^8 CFU/ml, for use in assays.

PROCEDURE:
The antifungal activities of the synthesized nanoparticles were assessed using the standard disc diffusion method described by Bauer et al [17], and modified according to clinical and laboratory standards institute guidelines.

1. A 250 ml quantity of potato dextrose agar was prepared with sterile distilled water and sterilized in an autoclave at 121°C and 15 lb pressure for 15 minutes.
2. The medium was allowed to cool to room temperature and was then poured into sterile Petri dishes, allowing it to solidify.
3. The fungal culture inoculum, adjusted to 0.5 McFarland standards, was swabbed over the medium using a sterile cotton swab.
4. Two sterile discs were placed on each Petri dish using sterile forceps, one disc for the positive control and the other for a combination assay. Samples (20 µl) and sample controls (methanol) were added to each sterile disc, as well as to the antibiotic disc (Amphotericin-B), before incubating at 27°C for 48 hours. This experiment was conducted in triplicate to prevent contamination.
5. Zones of inhibition were observed and measured with a ruler.

RESULT AND DISCUSSION

X-ray Diffraction Study (XRD)
Figure 1 Shows XRD patterns of copper ferrite samples synthesized with various Ag substitutions (1 wt %, 2 wt%, and 3 wt %) and annealed at 350°C for 3 hours are presented. The diffraction peaks align with international standard diffraction data (JCPDS number 36-1451), confirming the presence of Ag-doped $CuFe_2O_4$. The average particle size of Ag-doped $CuFe_2O_4$ nanoparticles was found to be approximately 21 nm. The peaks correspond with those of standard Ag-doped CuFe2O4 and display high crystallinity. The identified diffraction planes were (111), (220), (311), (400), (422), (511), and (440), corresponding to Bragg angles of 18.40, 30.00, 38.26, 44.09, 49.59, 58.22, and 62.22, affirming the formation of single-phase cubic spinel structures. No impurity peaks were observed, attesting to the samples' purity [18]. The slight differences in peak positions among the samples are attributed to the varying percentages of silver doping. Increased doping concentration influences the crystalline characteristics of the samples. The average nanoparticle size, calculated using the Debye-Scherrer equation [19] ,

$$D = \frac{0.89\lambda}{\beta\cos\theta}$$

is estimated at approximately 21 nm. The reflection peak positions for the doped powders are almost identical to those of the calcined material, suggesting that the fundamental structure of the nanoparticles is consistent with the bulk material.

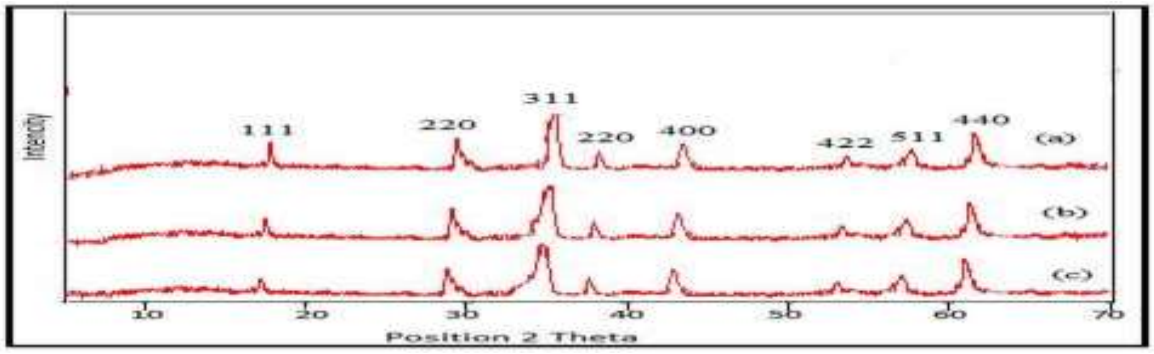

Figure 1 X-ray diffraction patterns for (a) 1 wt %, (b)2 wt% and (c)3 wt% Ag doped CuFe2O4 NPs calcinied at 350^0C.

FOURIER TRANSFORM SPECTROSCOPY (FTIR) CHARACTERIZATION:

FTIR spectroscopy was employed to identify the functional groups present in the ferrite composition. The FTIR spectra for the Ag-doped $CuFe_2O_4$ samples were recorded in the 4000-400 cm^{-1} range. An absorption band at approximately 3550 cm^{-1} indicates the presence of O-H groups. The IR spectra reveal two pronounced absorption bands within the 400-600 cm^{-1} range, characteristic of spinel structures, confirming the samples' spinel nature. Higher frequency bands are observed between 600-500 $cm^{-1,}$ while lower frequency bands are situated between 500-400 cm^{-1}, a common characteristic for all ferrites. The absorption bands at 600 cm^{-1} and 400 cm^{-1} were noted for all compositions, indicating the formation of a single-phase spinel structure involving tetrahedral (A) and octahedral sites [21]. The spectra exhibit two absorption peaks at 543 and 443 cm^{-1}, which correspond to the M-O stretching frequencies of ferrospinels. A characteristic band at 1373 cm^{-1} is attributed to the symmetric vibration of the NO_3 group, while peaks at 997 and 710 cm^{-1} indicate the presence of Fe ions in ferrites.

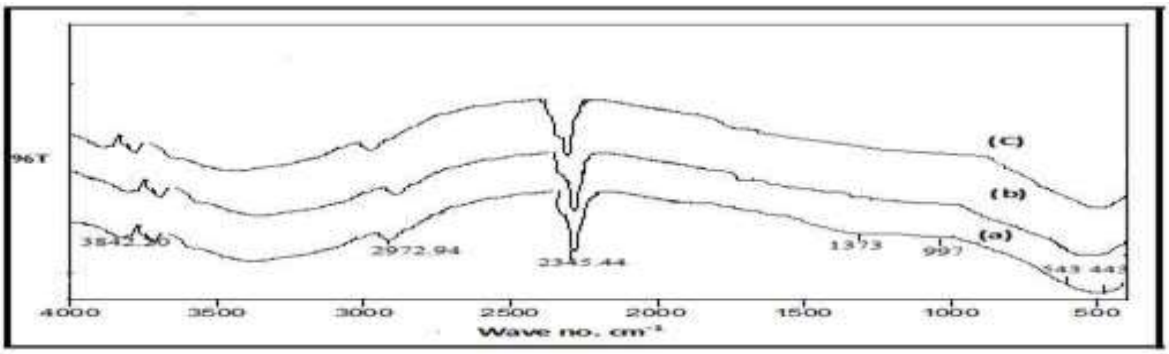

Figure 2 FTIR Spectra for (a) 1 wt% (b)2 wt% and (c) 3 wt% Ag doped CuFe2O4 NPs calcinate at 350^OC.
Transmission Electron Microscopy (TEM) Characterization

TRANSMISSION ELECTRON MICROSCOPY (TEM) CHARACTERIZATION:

The morphology and crystalline structure of undoped and Ag-doped $CuFe_2O_4$, calcined at 350°C for 3 hours, were further examined using TEM. The bright-field images of the samples demonstrate that both pure and Ag-doped $CuFe_2O_4$ nanoparticles are approximately 21 nm in size. The particle sizes derived from the XRD pattern correlate well with the TEM results. The selected area electron diffraction (SAED)

pattern indicates the crystalline nature and preferred orientation of the Ag-doped $CuFe_2O_4$ samples, consistent with the quartz structure indicated by the XRD results and the standard JCPDS data card.36-1451

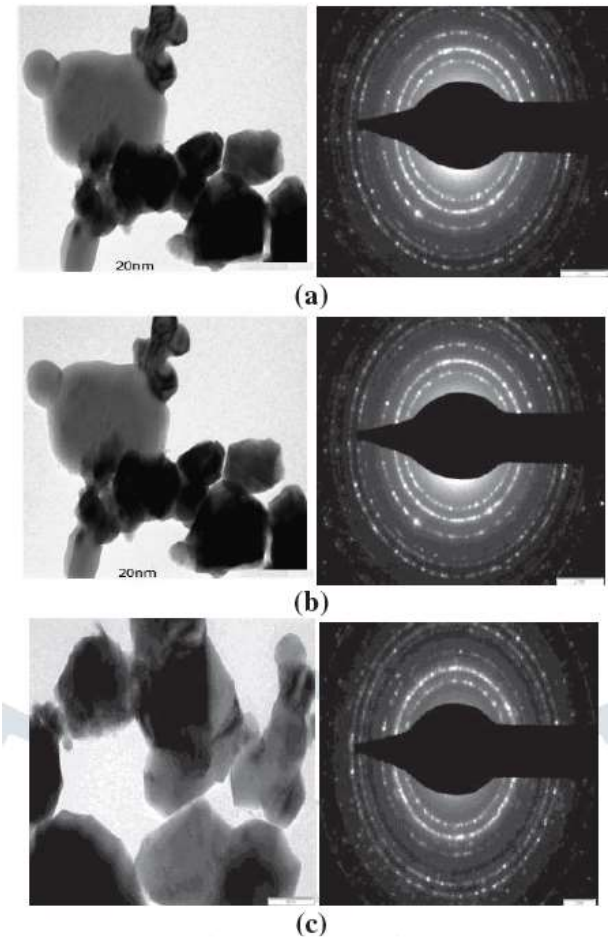

Figure 3 TEM images with corresponding SAED patterns of the (a) 1 wt % (b) 2 wt % and (c) 3 wt %Ag doped CuFe2O4 NPs calcinate at 350°C.

ANTIFUNGAL ACTIVITY

The antifungal efficacy of Ag-doped (1 wt%, 2 wt%, and 3 wt%) $CuFe_2O_4$ nanoparticles, calcined at 350°C, was evaluated using the disc diffusion method. The antimicrobial activities against three fungal pathogens, namely Aspergillus flaves and Aspergillus niger, were assessed. The zones of inhibition are documented in the data tables and figures. Results demonstrate that $CuFe_2O_4$ nanoparticles with silver doping exhibit greater antifungal activity than the pure $CuFe_2O_4$. The findings suggest that the doping process significantly enhances the antimicrobial properties of the nanoparticles. This report indicates that Ag-doped $CuFe_2O_4$ nanoparticles have the most effective antifungal behavior compared to their undoped counterparts. Results align with earlier studies indicating that transition metals boost antifungal activity. The data imply that active oxygen species generated from both pure and doped ferrite transition metal oxides can penetrate cell walls and impair cell division. Furthermore, doped samples show better inhibition than pure samples, reflecting outcomes better than previous reports [22]. Increased concentrations of doping correlate with heightened antimicrobial activity, corroborating past research on the antimicrobial effects of nanoparticles. As the concentration of doped metals increases in the culture medium, interactions between oxygen and dehydrogenase intensify, further enhancing antimicrobial effect [24].

International Journal of Environmental Sciences
ISSN: 2229-7359
Vol. 11 No. 2s, 2025
https://www.theaspd.com/ijes.php

Aspergillus Niger

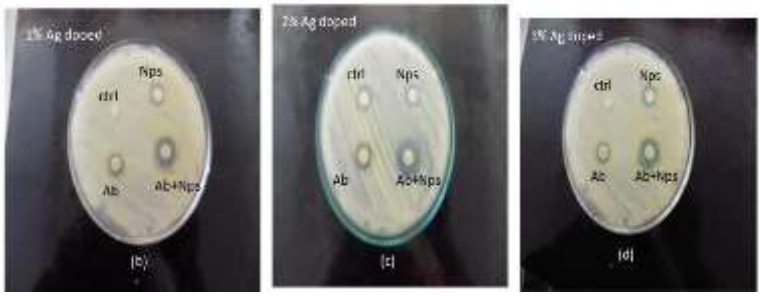

Figure 4 Zone of inhibition of the antifungal activity of (a) 1 wt%, (b) 2 wt% and (c) 3 wt% doped Ag in CuFe2O4,

Aspergillus Flaves

Figure 5 Zone of inhibition of the antifungal activity of (a) 1 wt% doped Ag, (b) 2 wt% and (c) 3 wt% doped Ag inCuFe2O4, against A. Flaves.

Fungal pathogenes	1wt% Ag doped	2 wt% Ag doped	3 wt% Ag doped
A. flavus	17mm	19mm	21mm
A. niger	15mm	18mm	20mm
Control	8mm	6mm	8mm

Table 1 Zone of inhibition of the antifungal activity of 1 wt%, 2 wt% and 3 wt% Ag doped CuFe2O4 against fungal pathogens.

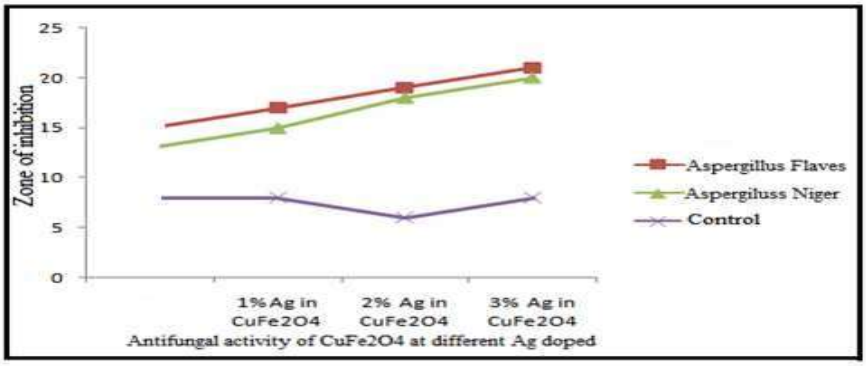

Figure 6 Antifungal activities of 1 wt%, 2 wt% and 3 wt% Ag doped CuFe2O4 against fungal pathogens

Fungal pathogens	1 wt% Ag doped	2 wt% Ag doped	3 wt% Ag doped
A.flavus			
Antibiotic	22mm	23mm	24mm
Antibiotic + Nps	23mm	24mm	25mm
A. niger			
Antibiotic	20mm	22mm	23mm
Antibiotic + Nps	21 mm	23 mm	25mm

Table 2 Zone of inhibition of the antifungal activity of 1 wt%, 2 wt% and 3 wt% Ag doped CuFe2O4 withAntibiotic

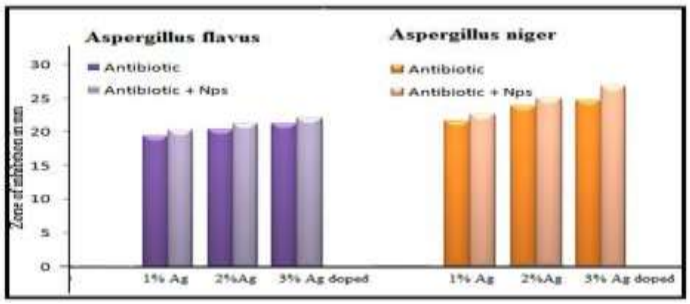

Figure 7 Antifungal activity of antibiotic and antibiotic + Nps against Aspergillus flavus and Aspergillus niger.

CONCLUSION

The study on the effect of 1 wt%, 2 wt%, and 3 wt% silver-doped copper ferrite synthesized through the sol-gel method indicated that XRD confirmed all peaks correspond to the single-phase spinel cubic structure without impurity from secondary phases of $CuFe_2O_4$. FTIR analyses demonstrated the presence of octahedral and tetrahedral sites within the spinel structure, while TEM images showed that most of the nanoparticles were spherical and some were agglomerated. The estimated particle size is 21 nm, corroborated by XRD and TEM analyses. Moreover, the antifungal assays indicated that the silver doping significantly enhances the inhibition zones at 3 wt% Ag-doped $CuFe_2O_4$ nanoparticles.

REFERENCES:

1. Stoimenov, P. and Klabunde, R. 2002. Metal oxide nanoparticles as bactericidal agents. Langmuir, 18(17): 6679-6686.
2. Kim, K., Sung, W., Moon, S., Choi, J. S., and Kim, G. 2008. Antifungal and mode of action of silver nanoparticles on Candida albicans. Biomaterials, 22(2): 235-242.
3. Cioffi, N., Torsi, L., Ditaranto, N., Tantillo, G., Ghibelli, L., Sabbatini, L., Zacheo, T., Alessio, M., Zambonin, P., and Traversa, E. 2005. Copper nanoparticle polymer composite with antifungal and bacteriostatic properties. Chemistry of Materials, 17(21): 5255-5262.
4. Liu, Y., He, L., Mustapha, A., Li, H. A., and Lin, M. 2009. Antibacterial activities of zinc oxide nanoparticles against Escherichia coli O157:H7. Journal of Applied Microbiology, 107(4): 1193-1201.
5. Sanpo, N., Berndt, C., Wen, C., and Wang, J. 2013. Transition metal-substituted cobalt ferrite nanoparticles for biomedical applications. Acta Biomater, 9(3): 5830–5837.
6. Sanpo, N., Berndt, C., and Wang, J. 2012. Microstructural and antibacterial properties of zinc-substituted cobalt ferrite nanopowders synthesized by sol-gel methods. Journal of Applied Physics, 112(8): 084333-084336.

7. Alimuddin, H., Shirsath, S. Meena, and S. Kotnala, R. 2013. Investigation of Structural, Dielectric, Magnetic and Antibacterial activity of Cu-Cd-Ni-FeO4. Journal of Magnetism and Magnetic Materials, 341(6): 148-157.
8. Parveen, A., Koppalkar, A., Patil, S., and Roy, A. 2013. Photocatalyst obtained by the solvothermal process using ionic liquid. Ionics, 19(5): 191-198.
9. Joshi, S., Kumar, M., Chhoker, S., Srivastava, G., Jewariya M., and Singh, V. 2014. Structural, Magnetic, Dielectric, and Optical properties of Nickel Ferrite Nanoparticles synthesized by Co-precipitation method. Journal of Molecular Structure, 1076: 55-62.
10. Hessin, M., Rashad, M., Barauy, K., and Ibrahim, I. 2008. Influence of manganese substitution and annealing temperature on the formation, microstructure, and magnetic properties of Mn-Zn ferrites. Journal of Magnetism and Magnetic Material, 320(9): 1615-1621.
11. Venkataraju, C., Sathish Kumar, G., and Sivakumar, K. 2010. Effect of Nickel on the electrical properties of Nanostructured Mn-Zn Ferrites. Journal of Alloys Compound, 498(2); 203-206.
12. Bayrakdar, H., Yalcin, O., Vural, S., and Esmer, K. 2013. Effect of different doping on structural, morphological, and magnetic properties of Cu-doped nanoscale spinel-type ferrites. Journal of Magnetism and Magnetic Material, 343(1): 86-91.
13. Ata-Allah, S., and Yehia, M. 2009. Physica B, 404: 2382-2388.
14. Ranjith Kumar, E., Jayaprakash, R., Sarala Devi G., and Reddy, P. 2014. Magnetic, Dielectric and sensing properties of Manganese substituted copper ferrite nanoparticles. Journal of Magnetism and Magnetic Material, 355(6): 87-92.
15. Brinker, J., and Scherer, W. Academic Press, San Diego, 1990.
16. Bauer, A., Kirby, W., Sherris, J., and Turck, M. 1966. Antibiotic susceptibility testing by a standardized single disk method. American Journal of Clinical Pathology, 45(4): 493-496.
17. Manikandan, A., Vijaya, J., Kennedy, L., and Bououdina, M. 2013. Structural, optical, and magnetic properties of Zn1-xCuxFe2O4 Nanoparticles prepared by microwave combustion method. Journal of Molecular Structure, 1035(13): 332-340.
18. Li, X., Hou, Y., Zhao, Q., and Wang, L. 2011. Journal of Colloid and Interface Science, 358: 102-108.
19. Labde, B., Sable, M., and Shamkumar, N. 2003. Structural Infrared studies of Ni1+xPbxFe2-xO4 system. Journal of Materials Letters, 57(11): 1651-1655.
20. Mohmad R., Rashad, M., Haraz, F., and Sigmund, W. 2010. Journal of Magnetism and Magnetic Materials, 322: 2058-2063.
21. Sanpo, N., Christopher, C., and Wang, J. 2012. Microstructural and antibacterial properties of zinc-substituted cobalt ferrite Nanopowders synthesized by sol-gel Method. Journal of Applied Physics, 112(8): 1-6.
22. Hranisavljevic, J., Dimitrijevic, N., Wurtz, G., and Wiederrecht, G. 2002. Photoinduced Charge Separation Reactions of J-Aggregates Coated on Silver Nanoparticles. Journal of American Chemical Society, 124(17): 4536-4537.
23. Sikong, L., Kongreong, B., Kantachote, D., and Sutthisripok, W. 2010. Photocatalytic activity and antibacterial behavior of Fe3+-doped TiO2/SnO2 nanoparticles. Energy Resources.